Int. J. of Applied Mechanics and Enginering, 2006, vol.11, No.3, pp.449-465

This paper was prepared on the Fourth International Tribology Conference ITC 2006

MODELING OF FRICTIONAL CONTACT PARAMETERS OF MECHANICAL SYSTEMS

J. ABDO*
Sultan Qaboos University
Mechanical and Industrial Engineering Department
P.O. Box 33, Al-khoud 123, SULTANATE OF OMAN
e-mail: jdabdo@squ.edu.om

It is well recognized that the contact stiffness, true contact area, and the contact force are among the key features in the study of friction system behavior. This paper presents the development of formulae for the mechanical component of dry-friction at the interface of two microscopic rough surfaces. Elastic deformation under the influence of the contact forces is considered. The elastic contact model formulation between interacting asperities is not assumed to occur only at asperity peaks, thus allowing the possibility of oblique contacts wherein the local contact surfaces are no longer parallel to the mean planes of the mating surfaces. It is shown that the approach enables the separation of the contact area into its normal and tangential projections and the contact force into its normal and tangential components. The mathematical model of contact is utilized to develop formulae for normal and tangential contact stiffness. The analytical method is used to estimate contact stiffness components. Contact parameter values for the sample are derived from the surface profile data taken from a *1.0 mm* by *10 mm* test area. The profile is measured using a Mahr profilometer. A computer program is written and used to analyze the profile data. The analysis yields the asperity density, average asperity radius, and the standard deviation for each test area.

Key words: contact area, contact force, and contact stiffness.

1. Introduction

Performance of mechanical systems with friction is greatly influenced by contact characteristics. An accurate estimation of the contact force and contact area in the interaction of rough surfaces is undoubtedly one of the most challenging problems. Harnessing contact problems will have wide-reaching benefits to the design of mechanical seals, surfaces for manufactured parts, as well as components in clutch, brake and engine systems. The formulae for contact force, stiffness and real area of contact that consider micro-contact between the asperities in the elastic range are developed.

It is recognized that surfaces are rough on a microscopic scale. As a result when two solid bodies are brought into contact, the real contact area will only be a fraction of the apparent macroscopic contact area. Most of the existing contact models are based on the presumption that the real contact area can be thought as the area composed of asperities of one solid body, which are squeezed against asperities of the other body (Greenwood *et al.*, 1992; Greenwood and Williamson, 1966; Bush *et al.*, 1975; Johnson, 1985). These asperities can deform elastically or plastically depending on the material and loading conditions. Early research efforts focused on plastic models on the premise that the real contact area is so small that the contact pressure exceeds the yield point. Abbot and Firestone (1933) proposed one of the earliest plastic models, described the real contact area as the area of geometrical intersection between a rough surface and a plane. Bowden and Tabor (1954) suggested a model by assuming that the load is supported by the plastic contact pressure, being equal to the flow pressure of the softer contacting material. Archard (1953) proposed a model in which asperity is covered with micro-asperities that in turn were covered with micromicro-asperities, and successfully produced the approximation that contact area was proportional to applied load. The elastic

* To whom correspondence should be addressed

models primarily rely on the Hertz theory of contact between two elastic bodies (Greenwood and Williamson, 1966; Greenwood and Tripp, 1967; Greenwood and Tripp, 1971; Hisakado, 1974; Bush *et al*., 1975; McCool, 1986). These models differ in their assumptions related to surface and asperity geometry and material properties. These extensions have included, for instance, the inclusion of the surface curvature effects (Greenwood and Tripp, 1967), allowance for non-uniform curvature of asperity summits (Hisakado, 1974) and the presumption of average elliptic parabolloidal representation of asperity (Bush *et al.*, 1975). While other works have advanced models for anisotropic materials (McCool, 1986). Elastic formulations of the asperities are developed considering the mechanical components, Bengisu and Akay (1997; 1999). The normal and the frictional forces are related to the normal and tangential velocities of two rough surfaces through the deformation of contact asperities.

In reality, each asperity will indeed be wholly elastic when the overall load is light, but then as the overall load is increased some asperities will start to enter the plastic regime. Increasing the load those asperities will ultimately become fully plastic and a local limit state will exist, whilst simultaneously the more heavily loaded elastic asperities will start to enter the plastic regime, Abdo and Farhang (2005) and Abdo (2005) In this paper, an elastic portion in the contact model of Abdo (2005) is extended to account for contact of two rough surfaces in which the effect of shoulder-to-shoulder asperity contact is addresses by way of the contact slope. This extension allows the development of equations for both normal and tangential contact forces, contact stiffness as well as the projection of normal and tangential contact areas in the elastic interaction of rough surfaces.

2. Consideration of contact between two rough surfaces

In the present formulation contact between interacting asperities is not assumed to occur only at asperity peaks, thus allowing the possibility of oblique contacts wherein the local contact surfaces are no longer parallel to the mean planes of the mating surfaces. Hence, the physical phenomenon is more realistically represented. The asperities experience elastic deformation and the nature of the load is such that adjacent contacting asperities do not influence each other on a surface during deformation. This assumption is valid for low to moderate values of contact pressure, which happens to also be the case when elastic interaction dominates. The statistical values of asperity height distribution and the average asperity summit radius are two important parameters in the representation of a rough surface. The statistical representation of an asperity is a quadratic asperity shape and may be represented by the following equation

$$y = f(\rho) = \rho^2 / 2\beta \tag{2.1}$$

where, β is the radius of curvature of the peak.

Two asperities of heights z_1 and z_2 on two mating surfaces are considered. The horizontal distance between the two vertical central lines of the two asperities is defined as the radial distance r and d denotes the separation of the mean planes of the asperity peaks of the two surfaces. The conditions of no contact, touch and interference may be represented by the following mathematical inequalities shown also in Fig.1.

$$\begin{aligned} z_1 + z_2 - 2f(r/2) &< d \qquad (\textit{no contact}), \\ z_1 + z_2 - 2f(r/2) &= d \qquad (\textit{touch}), \\ z_1 + z_2 - 2f(r/2) &> d \qquad (\textit{interference}). \end{aligned} \tag{2.2}$$

In view of a two-dimensional representation of interfering asperities the geometrical intersections of the asperities are used to define the interference slope. Therefore, as depicted in Fig.2, the slope of the line

defined by the two points of interactions with respect to the mean plane is the interference slope. Let the points of intersections be given by points A and B in Fig.2 with coordinates (ρ_A, y_A) and (ρ_B, y_B), respectively.

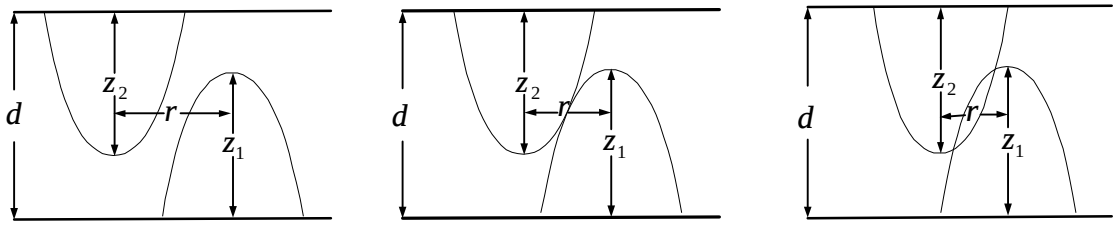

Fig.1. Representation of possible asperity interaction scenarios.

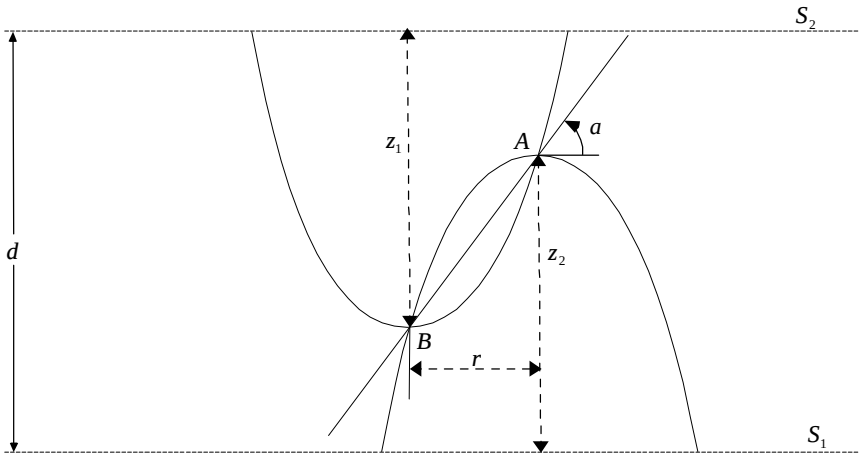

Fig.2. The contact slope of two asperities.

Therefore the slope may be written as

$$S_\alpha = \frac{y_A - y_B}{\rho_A - \rho_B} = \frac{r}{2\beta} \tag{2.3}$$

where, α is the angle between the line BA and the reference plane of surface S_1 as shown in Fig.2. The radial distance at which the two asperities touch (are tangent) may be calculated by equating

$$f(r/2) = r^2/8\beta, \tag{2.4}$$

whereas a comparison with Eq.(2.2) yields

$$r = \pm 2\sqrt{\beta(z_1 + z_2 - d)}. \tag{2.5}$$

It is noted here that a positive sign for r corresponds to the positive slope $(\alpha > 0)$ and a negative sign to the negative slope $(\alpha < 0)$. The Hertzian theory of contact employs the equivalent radius of curvature at the point of contact of the two bodies. For two bodies of radii of curvatures r_1 and r_2, the composite radius of curvature is given by

$$1/r_c = 1/r_1 + 1/r_2 . \tag{2.6}$$

Utilizing Eq.(2.1), the radius of curvature for two asperities of identical shape of the function in terms of the radial distance between an asperity mating surfaces and assuming identical statistics $(r = 2\rho)$ for the two surfaces may be given by

$$r_c = \frac{\beta}{2}\left(1 + \frac{r^2}{4\beta^2}\right)^{\frac{3}{2}} . \tag{2.7}$$

If we assume that r changes from zero, where the two asperities are aligned, to approximately 2β, where the asperities just touch, the average radius of curvature can be approximated $r_{ca} = \beta$.

Correct application of Hertzian contact equations requires the use of the interference along the normal to the contact area. Greenwood and Tripp (1971) define the interference w_1, as shown in Fig.3, normal to the mean planes. However, for the case under study involving oblique asperity contact, the interference is along the normal to the contact area, illustrated in Fig.3 to be approximately normal to the line joining asperity intersections. Denoting the interference by w and that due to GT as w_1, an approximate relation may be established between the interferences by utilizing the interference slope.

(a)

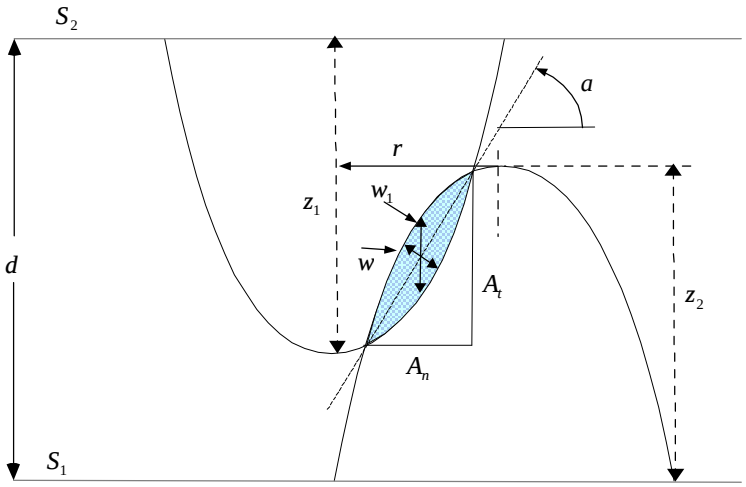

(b)

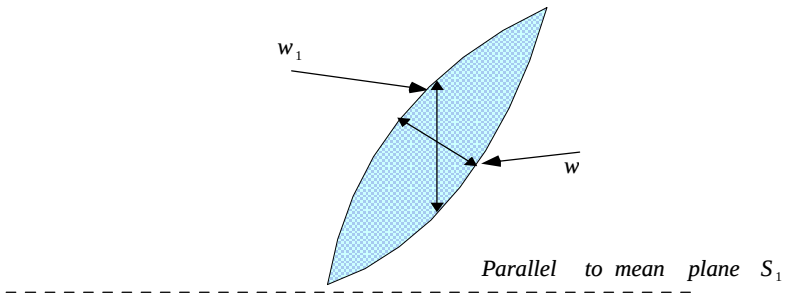

Fig.3. Projection of contact area onto its normal and tangential components.

$$w = w_1 \cos\alpha, \tag{2.8}$$

$$w_1 = z - d - 2f(r/2), \qquad z = z_1 + z_2, \tag{2.9}$$

$$S_\alpha = \tan\alpha, \tag{2.10}$$

then

$$\cos\alpha = \frac{1}{\sqrt{1+\tan^2(\alpha)}} = \frac{1}{\sqrt{1+S_\alpha^2}}. \tag{2.11}$$

Substituting Eqs (2.9) and (2.11) in Eq.(2.10)

$$w = (z - d - 2f(r/2))\left(1\Big/\sqrt{1+\frac{r^2}{4\beta^2}}\right). \tag{2.12}$$

The normal and tangential projections of the contact area A may also be written using the above definition of slope

$$A_n = A\cos\alpha = A\left(1\Big/\sqrt{1+S_\alpha^2}\right) = A\left(1\Big/\sqrt{1+\frac{r^2}{4\beta^2}}\right),$$

$$A_t = A\sin\alpha = A\left(S_\alpha\Big/\sqrt{1+S_\alpha^2}\right) = A\left(\frac{r}{2\beta}\Big/\sqrt{1+\frac{r^2}{4\beta^2}}\right). \tag{2.13}$$

Similarly, as illustrated in Fig.4, the contact force also consists of its normal and tangential components. The components may be related to the contact force and contact slope as follows

$$P_n = P\cos\alpha = P\left(1/\sqrt{1+S_\alpha^2}\right),$$
$$P_t = P\sin\alpha = P\left(S_\alpha/\sqrt{1+S_\alpha^2}\right) \tag{2.14}$$

where P is obtained by the Hertzian contact theory.

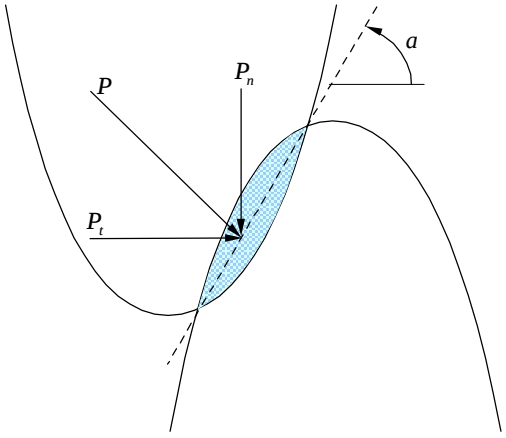

Fig.4. Contact force and its normal and tangential components.

Equations (2.12) to (2.14) are the required relations to derive macroscopic expectations of the contact area and its projections and contact force components. In the following sections the statistical estimations of total tangential and normal areas as well as tangential and normal forces between two rough surfaces are presented using the above relations.

3. Expected total normal and tangential contact areas and contact forces

The expected total normal contact area is the sum of the projections of local normal contact areas on the mean plane of the surfaces. The form proposed by GT is used to describe the normal projection of area as follows

$$\tilde{A}_n = \eta A \int_d^\infty A_{n0}(z-d)\phi(z)dz, \tag{3.1}$$

$$A_{n0} = 2\pi\eta \int_d^\infty A_n(w,r)rdr \tag{3.2}$$

where, A is the normal area, η the areal asperity density, assumed to be identical for both surfaces and $\phi(z)$ represents the probability density function of the sum of asperity heights (Greenwood and Tripp, 1971). Similarly, the expected total tangential contact area is the sum of the projections of local tangential contact areas.

$$\tilde{A}_t = \eta A \int_d^\infty A_{t0}(z-d)\phi(z)dz \tag{3.3}$$

where A_{t0} is defined by the following integral form

$$A_{t0} = 2\pi\eta \int_d^\infty A_t(\omega, r) r dr . \tag{3.4}$$

The integration of the normal component of the contact force over all possible local contact areas gives the total normal force (normal load) at the interface. Likewise, the integration of tangential component over all the local contact areas yields the tangential force.

$$\begin{aligned} \tilde{P}_n &= \eta A \int_d^\infty P_{n0}(z-d)\phi(z)dz, \\ \tilde{P}_t &= \eta A \int_d^\infty P_{t0}(z-d)\phi(z)dz \end{aligned} \tag{3.5}$$

where

$$\begin{aligned} P_{n0} &= 2\pi\eta \int_0^\infty P_n(w,r) r dr, \\ P_{t0} &= 2\pi\eta \int_0^\infty P_t(w,r) r dr. \end{aligned} \tag{3.6}$$

In calculating the tangential and normal contact forces, the contact force between two asperities is considered and statistically summed over all possible asperity interactions to obtain each component. In considering the elastic contact between asperities, the Hertz equation is used to relate the interference through asperity geometry and material property to force.

4. Elastic deformation

According to the Hertzian equations the contact area and contact load between two asperities having interference *w* are given by

$$A_0 = \pi\beta w, \tag{4.1}$$

$$P_0 = \frac{4}{3} E \beta^{\frac{1}{2}} w^{\frac{3}{2}} \tag{4.2}$$

where, β is the average equivalent composite radius of curvature and w is the interference along the normal of the contact area. Substituting Eq.(4.1) in Eq.(2.13)

$$A_n = \pi\beta w_1 \cos^2\alpha\,, \tag{4.3}$$

$$A_t = \pi\beta w_1 \cos\alpha \sin\alpha\,, \tag{4.4}$$

and substituting Eq.(4.2) in Eq.(2.14) yields

$$P_n = \frac{4}{3}E\beta^{\frac{1}{2}}(w_1\cos\alpha)^{3/2}\cos\alpha\,, \tag{4.5}$$

$$P_t = \frac{4}{3}E\beta^{\frac{1}{2}}(w_1\cos\alpha)^{3/2}\sin\alpha\,. \tag{4.6}$$

Substituting Eq (4.3) in Eq (3.2) and after appropriate substitutions, leads to the following

$$A_{n0} = 2\pi^2\eta\beta\int_0^{2\sqrt{\beta(z-d)}}\left(z-d-\frac{r^2}{8\beta}\right)\left(1\Big/\left(1+\frac{r^2}{4\beta^2}\right)\right)rdr\,. \tag{4.7}$$

Similarly, substitute Eq.(4.4) in Eq.(4.8) to obtain

$$A_{t0} = 2\pi^2\eta\beta\int_0^{2\sqrt{\beta(z-d)}}\left(z-d-\frac{r^2}{8\beta}\right)\left(1\Big/\left(1+\frac{r^2}{4\beta^2}\right)\right)\frac{r}{2\beta}rdr\,. \tag{4.8}$$

Similarly, substitute Eqs (4.5) and (4.6), respectively, in Eq.(3.6) and after appropriate substitutions we get

$$P_{n0} = \frac{8}{3}\pi E'\eta(\beta)^{\frac{1}{2}}\int_0^{2\sqrt{\beta(z-d)}}\left(z-d-\frac{r^2}{8\beta}\right)^{\frac{3}{2}}\left(1\Big/\left(1+\frac{r^2}{4\beta^2}\right)\right)^{\frac{5}{4}}rdr\,, \tag{4.9}$$

$$P_{t0} = \frac{8}{3}\pi E'\eta(\beta)^{\frac{1}{2}}\int_0^{2\sqrt{\beta(z-d)}}\left(z-d-\frac{r^2}{8\beta}\right)^{\frac{3}{2}}\left(1\Big/\left(1+\frac{r^2}{4\beta^2}\right)\right)^{\frac{5}{4}}\frac{r}{2\beta}rdr\,. \tag{4.10}$$

The integration of Eqs (4.7) and (4.8) gives

$$A_{n0} = 4\pi^2\eta\beta^3\left((d-\beta-z)\ln(\beta)+(\beta+z-d)\ln(\beta(\beta+z-d)-(z-d))\right), \tag{4.21}$$

$$A_{t0} = 8\pi^2\eta\beta^2\left(\beta(d-\beta-z)arctan\left(\frac{\sqrt{\beta(z-d)}}{\beta}\right)+\sqrt{\beta(z-d)}\left(\beta+\frac{2}{3}(z-d)\right)\right). \tag{4.22}$$

By substitution of Eqs (4.21) and (4.22) in Eqs (3.1) and (3.3), respectively, and presenting the integral forms for the expected total normal and tangential contact areas in normalized form, we get

$$A_n = 4\pi A\beta^3\eta^2\sigma^2\int_h^\infty\left((s-h)+\left(s-h+\frac{\beta}{\sigma}\right)\left(\ln\left(\frac{1}{\sigma}+\frac{s-h}{\beta}\right)\right)\sigma\right)\phi(s)ds\,, \tag{4.23}$$

$$A_t = 8\pi A\beta^2\eta^2\sigma^2\int_h^\infty\left(\beta\left(-s+h+\frac{\beta}{\sigma}\right)arc\tan\left(\frac{\sqrt{\sigma(s-h)}}{\beta}\right)+\sqrt{\sigma\beta(s-h)}\left(\frac{\beta}{\sigma}+\frac{2}{3}(s-h)\right)\right)\phi(s)ds \tag{4.24}$$

where σ is the standard deviation of asperity height sum distribution of the first and second surfaces. h is the dimensionless separation $(h=d/\sigma)$ and s is the dimensionless height $(s=z/\sigma)$. η is the areal density of asperity and $\phi(s)$ is the probability density function of the asperity height sum distribution. In this case, the Gussian probability distribution function is used.

$$\phi(s)=\frac{1}{\sqrt{2\pi}}e^{-\frac{s^2}{2}}\,. \tag{4.25}$$

In the above equations E' is the composite Young modulus of the two materials or friction film. It is defined as

$$\frac{1}{E'}=\frac{1-\nu_1^2}{E_1}+\frac{1-\nu_2^2}{E_2} \tag{4.26}$$

where E_1 and E_2 are the Young moduli of the surface films (materials) in contact. The elastic normal contact force per unit area can be written as follows

$$\tilde{P}_n = D_{ne}\,f_{ne} \tag{4.27}$$

where

$$D_{ne}=\frac{8}{3}\frac{\pi}{\sqrt{2\pi}}E'\eta^2\sqrt{\beta}\sigma^4\,, \tag{4.28}$$

$$f_{ne}=\int_h^\infty\left(\int_0^{2\sqrt{\beta(s-h)}}\left(s-h-\frac{r^2}{4\beta}\right)^{\frac{3}{2}}\left(1\Big/1+\frac{r^2}{4\beta^2}\right)^{\frac{5}{4}}rdr\right)\phi(s)ds\,. \tag{4.29}$$

The elastic tangential contact force per unit area can be written as follows

$$\tilde{P}_t = D_{te}\,f_{te}\,. \tag{4.30}$$

Note that the constants D_{ne} and D_{te} are identical. The f_{te} is expressed as

$$f_{te} = \int_{h}^{\infty} \left(\int_{0}^{2\sqrt{\beta(s-h)}} \left(s-h-\frac{r^2}{4\beta} \right)^{\frac{3}{2}} \left(1 \Big/ 1+\frac{r^2}{4\beta^2} \right)^{\frac{5}{4}} \frac{r^2}{2\beta} dr \right) \phi(s) ds \,. \tag{4.31}$$

It is noteworthy to mention that the integrals in Eqs (4.29) and (4.31) cannot be evaluated analytically. Instead, approximate analytical expressions are obtained using a truncated Taylor series expansion of the integrands. Eqs (4.23), (4.24), (4.27) and (4.30) are integrated numerically by changing the normalized separation h from *0* to *4*.

5. Contact normal and tangential stiffness

The contact of two asperities is shown in Fig.3. It may be represented by a spring in the normal and tangential directions for each asperity as shown in Fig.5. The normal contact stiffness per unit area is derived by differentiating the normal force $\tilde{P}_n$ in Eq.(4.27) with respect to the normal deformation of contacting asperities, $\delta = \sigma(s-h)$. The normal contact stiffness is

$$K_n = \frac{d\tilde{P}_n}{d\delta} = \frac{d\tilde{P}}{dh}\frac{dh}{d\delta} = -\frac{1}{\sigma}\frac{d\tilde{P}_n}{dh}, \tag{5.1}$$

and may be written as follows

$$K_n = H_n \, k_n \tag{5.2}$$

where

$$K_n = \frac{8}{3}\pi E' \eta^2 \sqrt{\beta}\sigma^3 A \int_{h}^{\infty} \left(\int_{0}^{2\sqrt{\beta(s-h)}} \left(s-h-\frac{r^2}{4\beta} \right)^{\frac{1}{2}} \left(1 \Big/ \left(1+\frac{r^2}{4\beta^2} \right) \right)^{\frac{5}{4}} r dr \right) \phi(s) ds \,, \tag{5.3}$$

$$H_n = \frac{8}{3}\pi E' \eta^2 \sqrt{\beta}\sigma^3 A \,. \tag{5.4}$$

The tangential contact load per unit area is derived by differentiating Eq.(4.30) with respect to r. The result is

$$k_t = \frac{\partial P_t}{\partial r} = \frac{4}{3} E' \beta^{1/2} \left(\frac{\partial (w_1 \cos\alpha)^{\frac{3}{2}}}{\partial r} \sin\alpha + (w_1 \cos\alpha)^{\frac{3}{2}} \frac{\partial(\sin\alpha)}{\partial r} \right). \tag{5.5}$$

The total tangential stiffness can be expressed as

$$K_t = \frac{8}{3} E' \beta^{1/2} \pi \eta^2 A \int_{h}^{\infty} \left(\int_{0}^{2\sqrt{\beta(s-h)}} k_t \; r \; dr \right) \phi(s) ds \,, \tag{5.6}$$

or

$$K_t = H_t k_t . \tag{5.7}$$

Notes that the constants H_n and H_t are identical and equal to *H*.

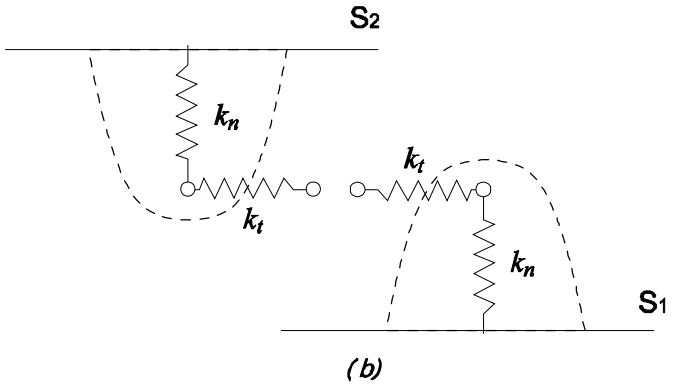

Fig.5. Representation of asperity interference.

6. Results and discussion

Figure 7 illustrates the relationship between the normal and tangential contact areas versus normalized separation. As expected both areas decrease by increasing separation and they are almost equal to zero at $h = 4$. The tangential contact area is slightly larger than the normal. The normal and tangential contact forces are shown in Fig.8. It should be noted that the results are only due to contacts corresponding to the positive slope. As shown in Fig.9a, when in static equilibrium, without the presence of an applied tangential force, the contact force due to the negative contact slope will be equal to that due to the positive slope. Therefore, the net tangential force on a surface is zero and the net normal force is twice that shown in Fig.9a.

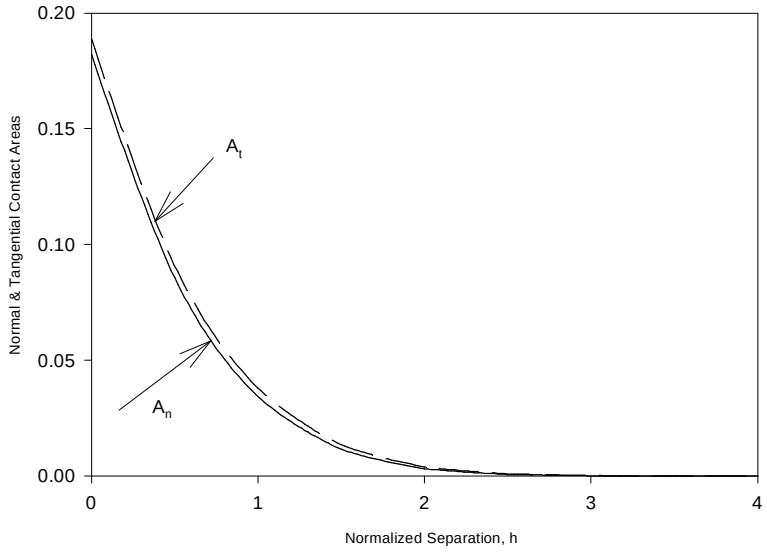

Fig.7. Normal and tangential projections of contact area vs. mean plane separation.

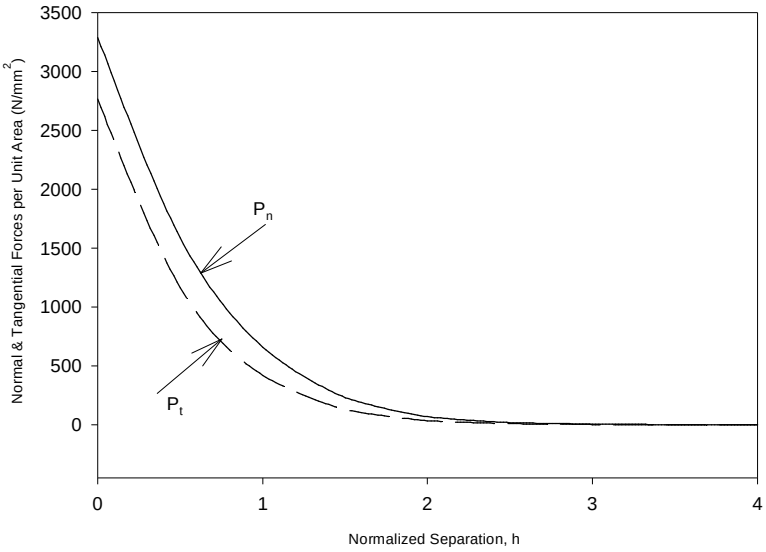

Fig.8. Normal and tangential components of contact force.

$$(P_t)_{net} = (P_t)_{\alpha^+} - (P_t)_{\alpha^-} = 0\,. \tag{6.1}$$

In the presence of an applied tangential force, the equilibrium condition dictates the net tangential force to be the equilibrating force. Therefore

$$P_{a_t} = (P_t)_{\alpha^+} - (P_t)_{\alpha^-}\,. \tag{6.2}$$

This latter case is presented schematically in Fig.9b as a positive bias in the macroscopic contact of the positive slope.

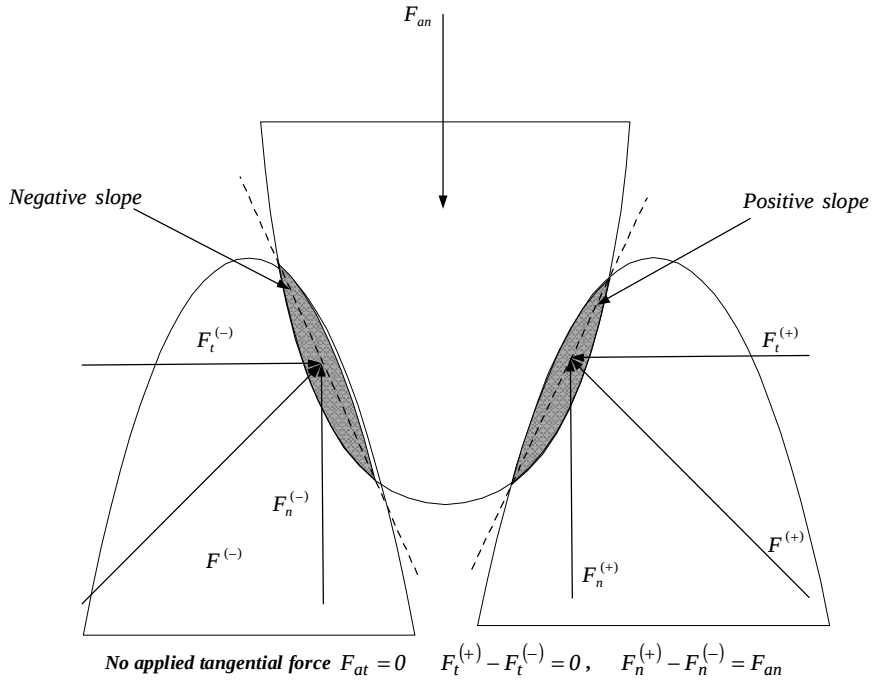

Fig.9a. Statistical representation of surfaces in contact and in the absence of an applied tangential force.

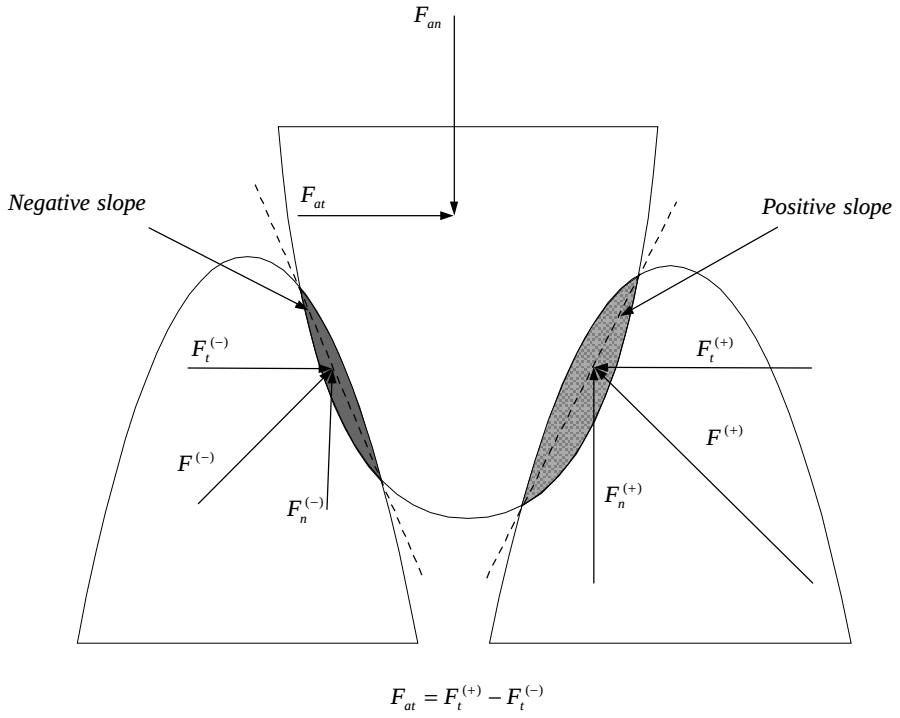

Fig.9b. Statistical representation of surfaces in contact and in the presence of an applied tangential force.

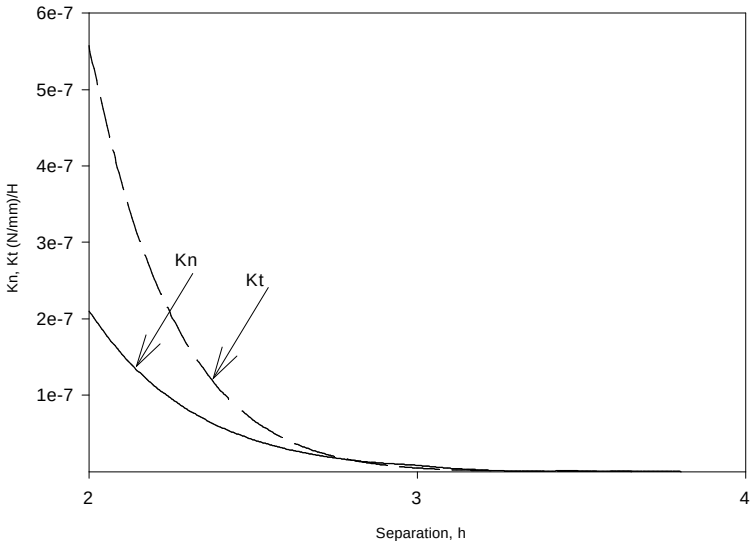

Fig.10. Normal and tangential Hertzian contact stiffness as a function of normalized separation for a $1mm \times 1mm$ sample $\left(H = 6.6 \times 10^{12}\right)$.

Figure 10 depicts the normalized normal and tangential contact stiffness for a $1mm \times 1mm$ sample versus the normalized separation for two rough surfaces, based on the information in Tab.1. Both normal and tangential contact stiffness decrease exponentially with separation, becoming negligible near $h = 4$. In the

range $h = 0$ to $h \approx 2.8$, the tangential contact stiffness is greater than the normal contact stiffness. But, in the range $h \approx 2.8$ to 4, the normal contact stiffness is greater than the tangential contact stiffness. The amount of interference has a greater effect on increasing tangential stiffness than normal stiffness, especially for separations less than $h = 2.8$, where the two are nearly equal.

Table 1. Greenwood and Williamson parameters and material properties for the aluminum sample.

asperity areal density $\eta\left(mm^{-2}\right)$	*16025*
Average asperity summit radius $\beta(mm)$	*0.006297*
Standered deviation of asperity height sum $\sigma(mm)$	*0.0081*
Composite modulus $E'\left(N/mm^2\right)$	*38700*
Poisson's ratio v	*0.33*
Shear modulus $G\left(N/mm^2\right)$	*14981*

Figures 11 and 12 illustrate the contact normal and tangential stiffness versus normal and tangential contact force, respectively. Both figures suggest that there exists near linear relationships between the stiffness and contact force, for relatively low to high contact forces. In this range

$$K_t = a_1 + a_2 P_n = b_1 + b_2 P_t,$$
$$K_n = c_1 + c_2 P_n = d_1 + d_2 P_t, \tag{6.3}$$

suggesting that similar near linear relationships hold between the normal and the tangential contact forces

$$P_n = A_1 + A_2 P_t,$$
$$A_1 = \frac{b_1}{a_2} - \frac{a_1}{a_2}, \qquad A_2 = \frac{b_2}{a_2}, \tag{6.4}$$

as well as between the normal and tangential contact stiffness

$$K_n = B_1 + B_2 K_t \tag{6.5}$$

where

$$B_1 = \frac{a_1 c_2}{a_2} - c_1, \qquad B_2 = \frac{c_2}{a_2}. \tag{6.6}$$

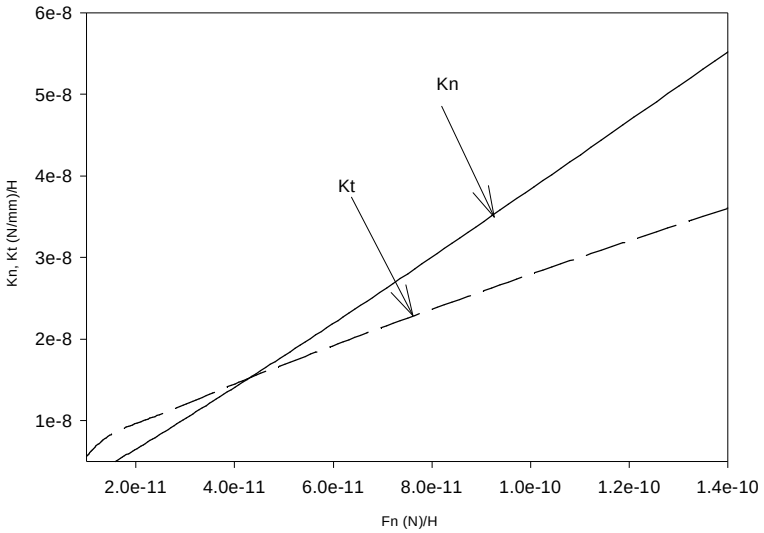

Fig.11. Normal and tangential Hertzian contact stiffness as a function of normal load for a $1mm \times 1mm$ sample $\left(H = 6.6 \times 10^{12}\right)$.

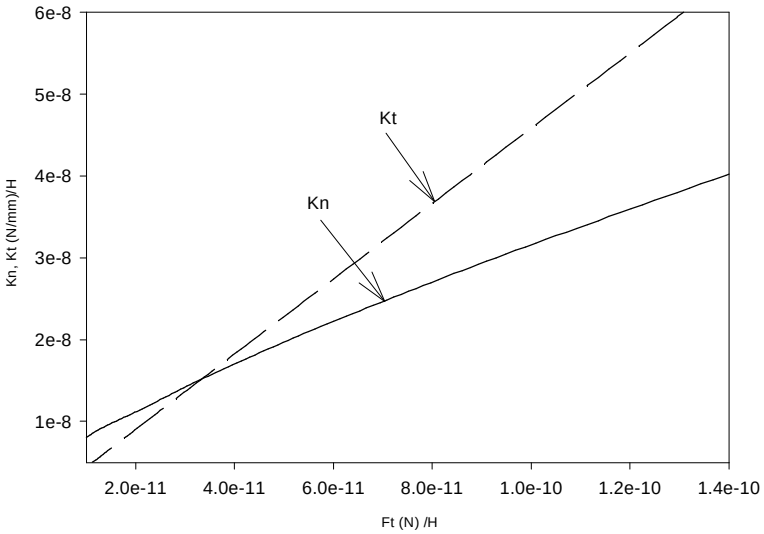

Fig.12. Normal and tangential Hertzian contact stiffness as a function of tangential load for a $1mm \times 1mm$ sample $\left(H = 6.6 \times 10^{12}\right)$.

7. Conclusions

The contact theories presented in this work have two important features: the interaction of two rough surfaces instead of one rough surface with a perfectly flat one and allowing the possibility of oblique contacts at the shoulders of the interacting surface asperities. The normal and tangential contact areas, contact loads and contact stiffness of rough surfaces under static conditions without an externally applied tangential force were formulated considering elastic deformations.

Nomenclature

A – contact area
A_n – normal projection of the contact area
$\tilde{A}_n$ – expected total normal contact area
A_{n0} – local normal contact areas
A_t – tangential projection of the contact area
$\tilde{A}_t$ – expected total normal tangential area
A_{t0} – local tangential contact areas
d – mean plane separation
E – Hertz elastic modulus
E' – equivalent (composite) elasticity modulus
h – separation based on surface heights
K_n – normal contact stiffness
K_t – tangential contact stiffness
P – contact force
P_n – normal projection of the contact force
$\tilde{P}_n$ – normal component contact force
P_{n0} – local normal contact force
P_t – tangential projection of the contact force
$\tilde{P}_t$ – tangential component contact force
P_{t0} – local tangential contact force
r – radial distance
w – interference
z – height of asperity measured from the mean plane of asperities
β – radius of curvature of the asperity peak
$\phi(z)$ – density function
η – asperity areal density
σ – standard deviation of surface heights

References

Abbott E.J. and Firestone F.A. (1933): *Specifying surface quantity-method based on accurate measurement and comparison*. – Mech. Eng., vol.55, pp.569-577.

Abdo J. (2005): *Experimental technique to study tangential to normal contact load ratio*. – Tribology Transactions, vol.48, pp356-365.

Abdo J. and Farhang K. (2005): *Elastic-plastic contact model for rough surfaces based on plastic asperity concept*. – International Journal of Non-Linear Mechanics, vol.40, pp.495-506.

Archard J.F. (1953): *Contact and rubbing of flat surfaces*. – J. Appl. Phys., vol.24, No.8, pp.981-988.

Bengisu M.T. and Akay A. (1997): *Relation of dry-friction to surface roughness*. – Journal of Tribology, vol.119, pp.18-25.

Bengisu M.T. and Akay A. (1999): *Stick-slip oscillations: dynamic of friction and surface roughness*. – J. Acoust. Soc. Am., vol.105, pp.194-205.

Bowden F.P. and Tabor D. (1954): *Part I. Friction and Lubrication of Solids*. – Oxford University Press.

Bowden F.P. and Tabor D. (1964): *Part II. Friction and Lubrication of Solids*. – Oxford University Press.

Greenwood J.A. and Williamson J.B. (1966): *Contact of nominally flat surfaces*. – Proc. Roy. Soc. (London), vol.A295, pp.300-319.

Greenwood J.A. and Tripp J.H. (1967): *The elastic contact of rough sphere*. – ASME J. of Appl. Mech., vol.34, pp.153-159.

Greenwood J.A. and Tripp J.H. (1971): *The contact of two rough nominally flat rough surfaces*. – Proc. Instn. Mech. Eng., vol.185, pp.625-633.

Greenwood J.A. and Singer H.M. Polack H.R. (Eds.) (1992): *Fundamentals of Friction, Macroscopic and Microscopic Processes*. – Dordrecht: Kluwer.

Bush A.W., Gibson R.D. and Thomas T.R. (1975): *The elastic contact of a rough surface*. – Wear, vol.35, pp.87-111.

Hisakado T. (1974): *Effect of surface roughness on contact between solid surfaces*. – Wear, vol.28, pp.217-234.

Johnson K.L. (1985): *Contact Mechanics*. – Cambridge University Press, Cambridge.

McCool J.I. (1986): *Predicting microfracture in ceramics via a microcontact model*. – ASME Journal of Tribology, vol.108, pp.380-386.

Received: May 15, 2006

Revised: June 24, 2006